7th Conference on Sustainability in Civil Engineering (CSCE'25)
(An International Conference)
Department of Civil Engineering
Capital University of Science and Technology, Islamabad Pakistan

NUMERICAL BEHAVIOR OF STEEL SPACE FRAME UNDER INCREMENTAL SEISMIC LOADS

[a] Kamran Shaukat*, [b] Muhammad Fahim

a: Department of Civil Engineering, UET Peshawar, Peshawar, Pakistan. cekamranshaukat@gmail.com
b: Department of Civil Engineering, UET Peshawar, Peshawar, Pakistan. drfahimuet@gmail.com
* Corresponding author

Abstract- Space frames are structural systems composed of linear elements arranged in a three-dimensional configuration to efficiently transfer loads. However, they exhibit complex dynamic behavior during earthquakes, particularly in seismically active regions such as Japan, China, and the United States. Notably, the 2013 Lushan earthquake caused severe damage to multiple structures, including three gymnasiums with space frame roofs. The destruction and collapse of long-span spatial structures are usually due to the large plastic deformation of the members. How to avoid bending and buckling due to the damage of the member under earthquake load is the key point in the design. This study investigates the elastic and plastic response of space frames using the finite element software ABAQUS. The structural model is assumed to be located in Abbottabad, Pakistan, a region with notable seismic activity. Incremental Dynamic Analysis (IDA) of a space frame was performed under the Chi-Chi (1999) earthquake record with progressively increasing intensity levels. Yielded Element Ratios and integration point evaluations was used to assess the yielding of members and section points. The findings provide a better understanding of how space frames behave under incremental seismic loads and give a brief understanding of performance-based design of space frames.

Keywords- Incremental Dynamic Analysis, Seismic Response, Space Frame, Yielding Behavior

1 Introduction

Single-layer space frames, known as lattice shells, can take the form of either flat or curved surfaces are widely used in the design of large-span public buildings such as sports arenas, exhibition pavilions, museums, and transportation terminals [1]. Their intricate geometries and interconnected joints make them vulnerable to various forms of damage during earthquakes [2]. The importance of comprehending the response of space frame is highlighted by various well-known structural collapses of space frames in the previous incidents. including Bucharest Dome [2], Hartford Civic Center Coliseum [3], Lushan and Baoxing gymnasium [4], [5]. Significant structural damage was observed in the Lushan and Baoxing gymnasiums during the 2013 Lushan earthquake such as buckling, joint failures, strength degradation, and member fractures [4], [5].

Large-span space structures in the form of reticulated domes are widely used in large-scale public buildings. Understanding the behavior of these structures under seismic loading is critical due to their susceptibility to complex failure mechanisms i.e. plastic hinge formation, member buckling, and progressive collapse [4], [6]. In order to have a better understanding of its mechanical performance and verify the collapse mechanism of space frame and failure patterns of the members a shaking table test was performed and a comparison between the experimental and numerical results obtained using the finite element software ABAQUS was made and a satisfactory agreement was found [7]. A theoretical strut model was introduced with the aim of increasing computational efficiency, The results were verified with experimental results [3], [7] confirming the reliability of numerical simulations. Zhi et al studied the failure modes due to instability and strength failures using a numerical model [8]. Furthermore, Different mitigation strategies have been tested to improve the seismic performance of steel space frames. Approaches such as viscous dampers [9], 3D base isolator [10], and buckling-restrained

braces (BRBs) [11] have been found effective in reducing damage, controlling deformation, and enhancing overall stability under seismic loading.

In this study, the plastic behavior of single-layer space frame, commonly referred to as reticulated dome. The structure is assumed to be located in Abbottabad, Pakistan. The region of high seismicity influenced by the Indus Kohistan thrust, which features active reverse and strike-slip fault mechanisms [19]. The dome configuration is based on a model previously studied by Zhi et al. in his detailed numerical study and was designed according to Chinese building codes [8]. A finite element model is developed in ABAQUS to simulate and analyse the initiation and progression of yielding, the formation of plastic zones, and the overall seismic resilience of the reticulated dome.

2 Research Methodology

The Chi-Chi (1999) earthquake was selected based on seismic geology of the area. To represent the seismic demand, a scenario-based Maximum Considered Earthquake (MCER) response spectrum corresponding to Site Class D was created. A Finite element model of the dome was developed using Q235B structural steel with uniform circular hollow sections. Rayleigh damping and non-structural mass were used to incorporate the corresponding effects on dynamic behavior of the dome. ABAQUS B32 beam element was used in the model, with two integration points per element and each integration point consists of four section points where stresses and strains were evaluated. Yielding at individual points was used to compute the Yielded Element Ratio (YER), defined as the ratio of elements in which yielding occurred at certain section points to the total number of elements. To distinguish the extent of plasticity, terms such as 1P, 5P, and 8P were used indicating that 1, 5, or all 8 section points in an element had yielded, respectively.

2.1 Numerical Model

The proposed numerical model represents a single-layer reticulated dome with a span of 40 meters and a rise-to-span ratio of 1/3 as shown in (Figure 1a). Structural steel was used as the material, with properties including a Poisson's ratio of 0.3, yield strength of 235 MPa, mass density of 7850 kg/m³, and an elastic modulus of 206 GPa. The corresponding yield strain was taken as 0.0015. The material's ultimate tensile strength ranged from 370 to 500 MPa, with a minimum elongation of 26%, in this study the elastic and hardening part of the curve has been taken for the sake of calculations and no damage or fracture was considered. To capture the plastic behaviour, a stress–strain curve was defined and applied in the model, as shown in Figure 1b. A uniform circular hollow section (CHS) pipe with outer diameter of 114 mm and 4 mm thickness was assigned to all the frame members including ring, radial, and diagonal members of the dome. Structural nonlinearity was modelled at the section point level. Roof mass of 200 kg/m² was applied as a non-structural mass at the nodes to all nodes that were not subject to boundary conditions. Rayleigh damping was applied with a damping ratio of 0.5. The first natural frequency of the dome was evaluated after modal analysis to be 2.55 Hz. The Raleigh constants were calculated the value of α and β were 0.7997 and 0.002.

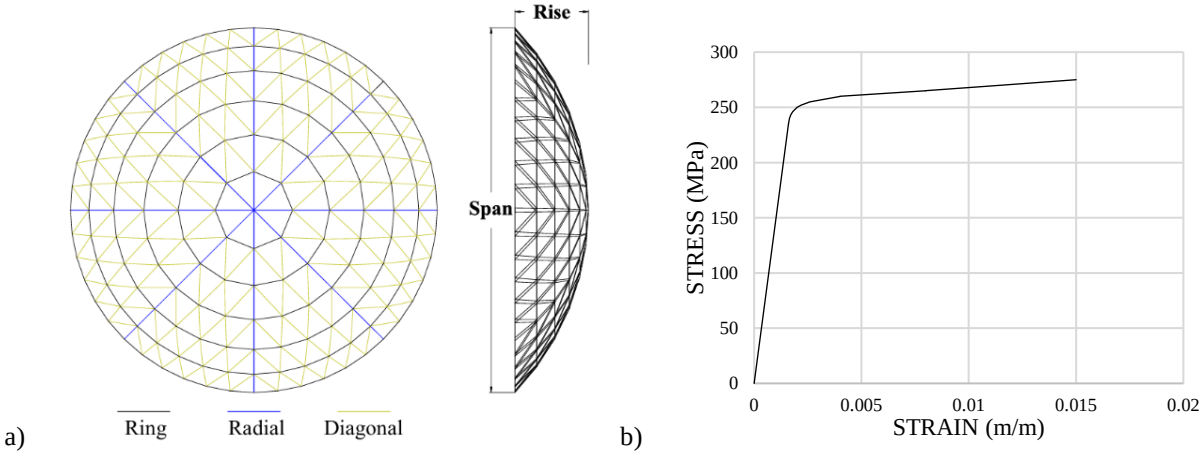

Figure 1: Details of the model, a. Geometry of the Kiewit-8 dome, b. stress strain curve of material model

2.2 Ground Motion Selection and Modification

The Chi-Chi (1999) earthquake ground motion was selected due to its reverse faulting mechanism, long duration, and moment magnitude of 7.6 on the Richter scale. These characteristics align with the regional seismicity and aligns to the Kashmir 2005 earthquake. The ground motion record was downloaded from the PEER ground motion database. The 3D ground motion record was first resampled from a time step of 0.004 seconds to 0.02 seconds. The first and last 0.05% of the ground motion energy were trimmed top remove low-impact tails. As a result, the total duration of the record was reduced from 150 seconds to 109 seconds. A comparison of the response spectrums before and after these modifications confirmed that the spectral characteristics were preserved. The comparison between the actual and modified time histories, along with their corresponding response spectrums are shown in (Figure2a, 2b).

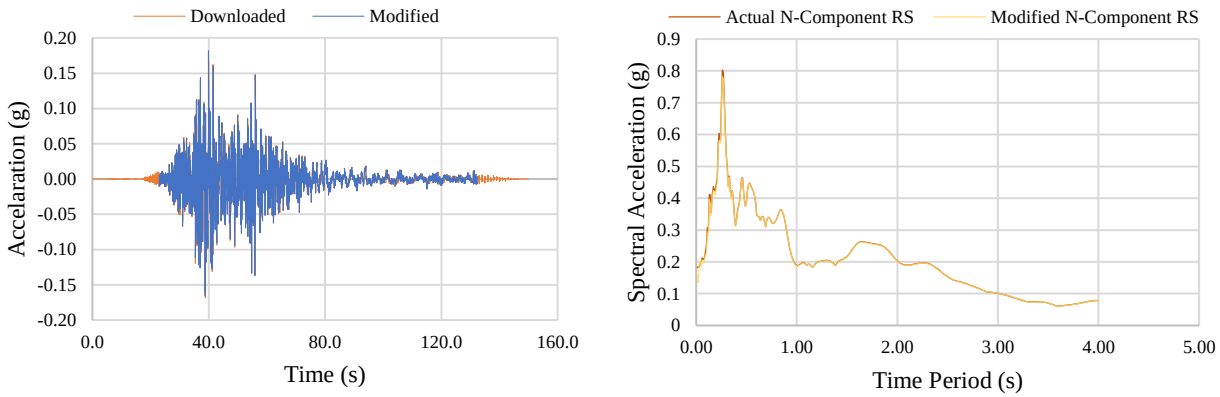

a) b)

Figure 2: N-Component before and after modifications, a. Time history, b. Response spectrum

2.3 Scaling of Ground motion

A scenario-based seismic hazard was considered in accordance with the Pakistan Building Code (PBC) 2021, corresponding to a 20% probability of exceedance in 50 years and a return period of 225 years. Maximum Considered Earthquake Risk (MCER) level, response spectrums were developed following the procedures outlined in Chapter 11 of ASCE 7-16 for both horizontal and vertical ground motions. These spectrums were then used to scale the selected ground motion components, ensuring consistency with the target hazard level at the site. The scale factors for horizontal and vertical components were calculated as 1.73 and 3.62. (Figure 3a) presents the scaled and unscaled horizontal ground motion spectra alongside the corresponding target hazard spectrum, while (Figure 3b) illustrates the comparison for the vertical component with its respective target spectrum.

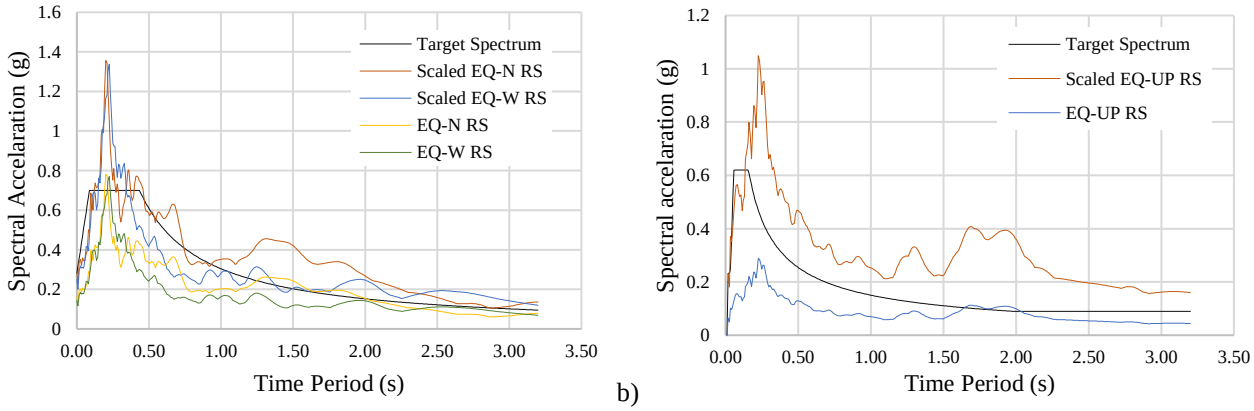

a) b)

Figure 3: Description of scaled, unscaled and target response spectrums, a. Horizontal, b. Vertical

2.4 Incremental Dynamic Analysis

Incremental Dynamic Analysis (IDA) was employed to evaluate both the elastic and inelastic behavior of the reticulated dome under increasing seismic intensity. The modified and scaled 3D ground motion were expressed in units of g (Figure. 4) and amplitudes were applied incrementally at seven levels, ranging from $0.5g \times A_{x,y,z}(t)$ to $1.5g \times A_{x,y,z}(t)$, where $A_{x,y,z}(t)$ denotes the 3D components of modified and scaled ground motion acceleration. At each intensity level, the structural response was assessed in terms of yielding initiation and plastic zone development.

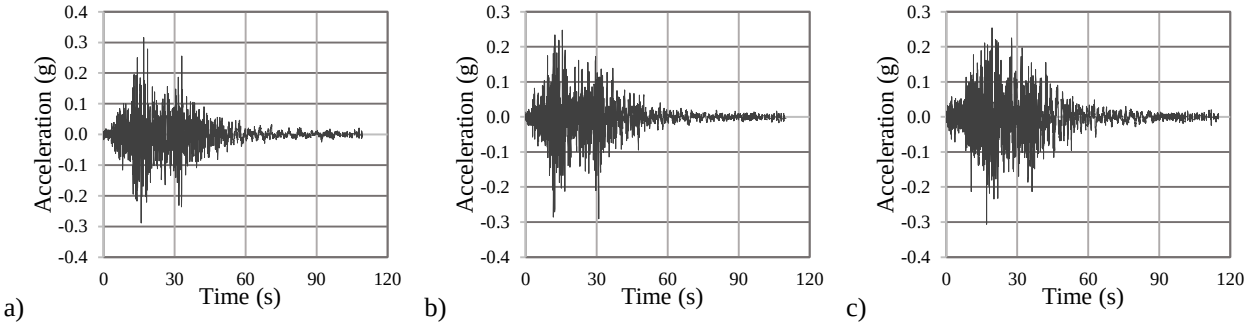

Figure 4: Details of Chi-Chi (1999) 3D ground motion, a. N-Component, b. W-Component, c. UP-Component

3 Results

The structural response has been evaluated in terms of yielded element ratios. A comparison between 1P and 5P, as well as between 5P and 8P, is made. The significance of assigning such a criterion lies in understanding the level of plasticity that occurs at a single element and evaluating if there is still elastic energy left in the section at as some parts of the section can deform elastically while others have already yielded. Response acceleration of the top node at three different intensity levels are evaluated, and Fourier transforms are conducted to study frequency content and amplitudes. In the last section, the progression of yielding has been discussed and described at four different intensities.

3.1 Structural Response

The structure remained elastic at 0.5g and started yielding when the intensity of the ground motion was increased to 0.6g and only two elements were yielded according to 1P yield element ratio. As shown in (Figure 3a), the 1P yield element ratio exhibits the earliest and most rapid increase, indicating early initiation of yielding under less restrictive conditions. At 1.0g, the 1P yield element ratio reaches approximately 0.19, while the 5P yield element ratio is 0.11, which is 44% lower, indicating delayed yielding under stricter criteria. At an intensity of 1.5g, the 1P ratio increases to 0.40, while the 5P yield element ratio remains 0.25, about 38% lower. From 0.6g to 1g, the 1P yield element ratio increases by 0.19, while the 5P ratio increases to 0.11, indicating a 44% slower growth. Within the higher intensity range from 1 to 1.5g, the 1P ratio grows by an additional 0.21, while the 5P yield element ratio increases by only 0.14, reflecting a 32% slower rate, continuing the trend of delayed yet accelerating yielding under stricter conditions.

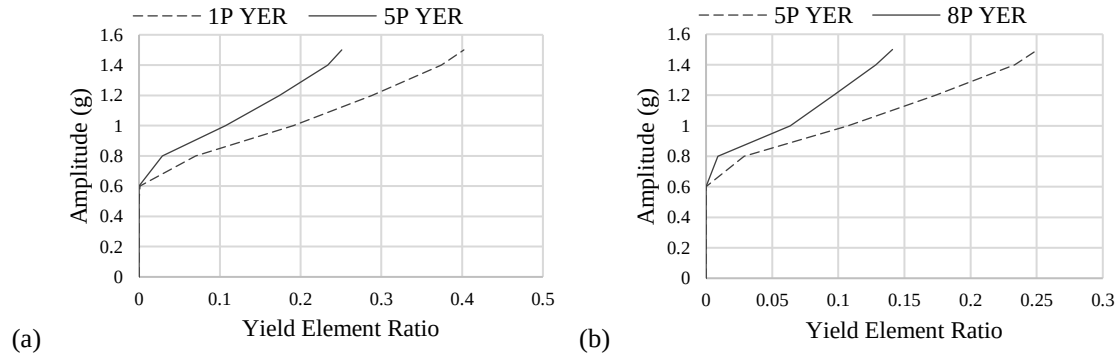

Figure 5: Comparison of Yield Element Ratios of the structure at increasing amplitudes

As shown in (Figure 3b), comparison between 5P, and 8P yield element ratios reveals a progressively delayed yielding behavior. At 0.8g, the 8P yield element ratio is approximately 87.1% lower than the 1P ratio and 68.6% lower than the 5P yield element ratio. At 1.0g, the 8P ratio remains 66.7% lower than the 1P ratio and 40.5% lower than the 5P ratio. At the intensity of 1.5g, the 8P ratio reaches a value 64.9% lower than the 1P ratio and 43.8% lower than the 5P yield element ratio, while the 5P ratio is 37.6% lower than the 1P ratio.

3.2 Acceleration Response

The acceleration response of the top node at increasing intensities was evaluated. The peak acceleration in the x-direction rose by 92.4% between 0.5g and 1.0g, and by 23.1% between 1g and 1.5g (Figure 4a), while in the y-direction the peak acceleration increased by 79.6% and 14.0%, respectively (Figure 4c). The vertical peak acceleration nearly doubled, increasing by approximately 99.6% from 0.5g to 1.0g and by 49.6% from 1g to 1.5g (Figure 4e). While the percentage gains decreased at higher amplitudes across all directions, the absolute amplification in peak acceleration at the top node remains persistent. Fourier analysis of the acceleration time histories revealed a slight but consistent shift in dominant frequencies. For the x-direction, the frequency corresponding to the peak Fourier amplitude decreased from 4.58 Hz at 0.5g to 4.37 Hz at 1.5g (Figure 4b), reflecting a softening response. The y-direction displayed a relatively stable dominant frequency of 4.48 Hz reducing to 4.46 Hz (Figure 4d). The vertical direction exhibited the highest frequency content, with dominant pepaks at 11.76 and 11.73 Hz. (Figure 4f).

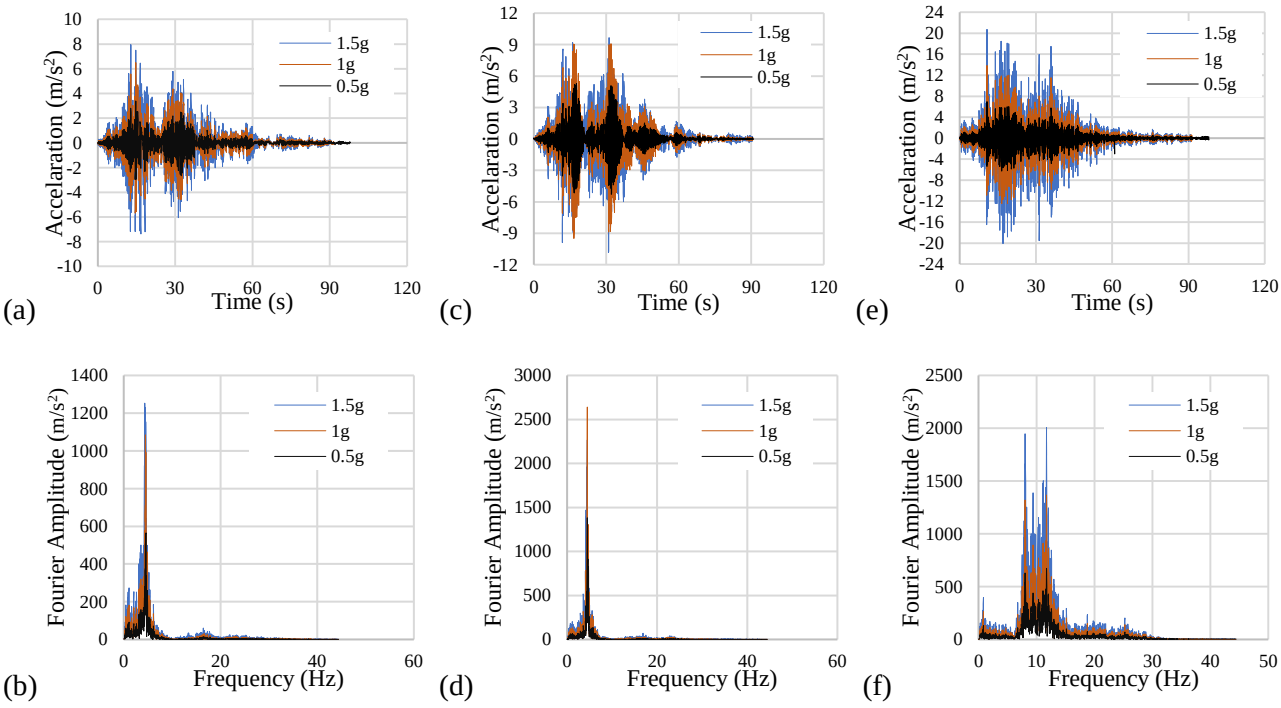

Figure 6: Acceleration response at the top node and corresponding Fourier transform at different amplitudes

3.3 Element Response

The yielding behavior of the dome under increasing seismic amplitudes is shown in (Figure 5a–d). Initial yielding occurred at 0.6g in two ring members having 1P yielded elements (0.0011). At 0.8g, diagonal members around radial members in the outermost ring yielded, with 1P, 5P, and 8P yielded element ratios of 0.07, 0.03, and 0.01, respectively. Members in the middle ring were partially yielded. When the intensity increased to 1.0g, the yielding spread among the diagonal elements of the second and outermost rings, with 1P, 5P, and 8P ratios rising to 0.19, 0.11, and 0.06. A small number of elements in ring members partially yielded, while no yielding was observed in radial members (Figure 5a). At 1.5g, most

of the diagonal elements in the outer rings had yielded, with ring elements on the middle and outer ring members showing 1P, 5P, and 8P values of 0.40, 0.25, and 0.14.

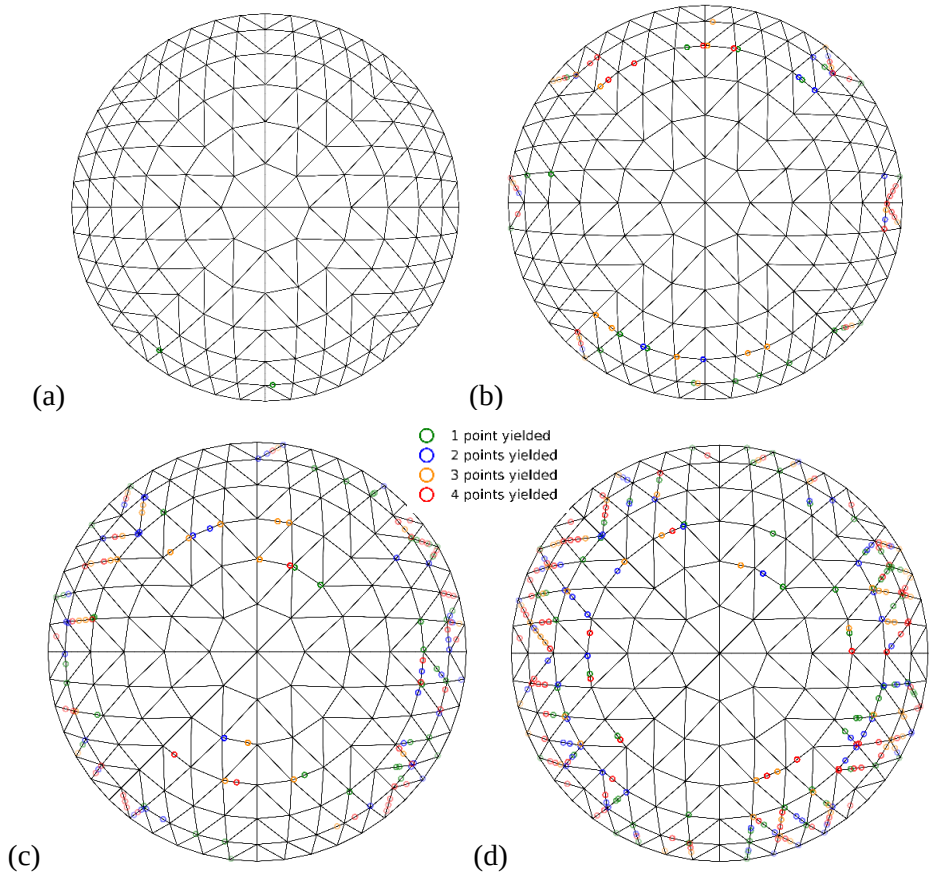

Figure 7: Progress of yielding at integration points with increasing intensities, a. 0.6g, b. 0.8g, c. 1.0g, d. 1.5g

4 Practical Implementation

The study investigated the elastic and plastic behavior of steel space frames, focusing on single-layer reticulated domes under seismic loading. It was evaluated how localized yielding initiates and spreads, affecting overall structural stability. The findings contribute to performance-based seismic design, enhancing the safety of long-span steel structures in earthquake-prone regions.

5 Conclusion

Following conclusions can be drawn from the conducted study:

1. As the seismic intensity increased, yielding propagated from the outer diagonal members toward the middle rings, while radial members remained mostly elastic even at 1.0g. This radial damage gradient reveals the directional nature of force transmission in reticulated dome geometries.
2. The choice of yield criteria such as elements yielding at 1, 5, or all 8 section points affects how the extent of yielding are interpreted. While 1P yield element ratio detects early damage, 8P yield element ratio captures severe yielding, highlighting the importance of multi-level criteria in evaluating damage states.
3. With increasing seismic amplitude, the dominant frequencies of the top node consistently decreased in all directions, primarily due to progressive stiffness degradation and energy dissipation resulting from structural yielding.

Future studies should incorporate modal projection methods and soil-structure interaction to fully capture realistic behavior and experimentally validate simulation results with models under shake table testing, especially to study failure modes in different configurations.

Acknowledgment

I am deeply grateful to my parents for their unwavering support, encouragement, and prayers throughout this journey. I would also like to express my sincere thanks to Dr. Khan Shahzada for generously sharing his PhD dissertation, which greatly contributed to this research. My heartfelt appreciation goes to Dr. Muhammad Faheem for his continuous guidance and valuable insights throughout the course of this work.

References

[1] T. T. Lan, "Space Frame Structures".
[2] J. Yan, F. Qin, Z. Cao, F. Fan, and Y. L. Mo, "Mechanism of coupled instability of single-layer reticulated domes," *Eng. Struct.*, vol. 114, pp. 158–170, May 2016, doi: 10.1016/j.engstruct.2016.02.005.
[3] Y. Ding, Z.-T. Chen, L. Zong, and J.-B. Yan, "A theoretical strut model for severe seismic analysis of single-layer reticulated domes," *J. Constr. Steel Res.*, vol. 128, pp. 661–671, Jan. 2017, doi: 10.1016/j.jcsr.2016.09.022.
[4] G. Nie, C. Zhang, D. Li, Q. Chen, and Z. Wang, "Collapse of the spatial double-layer cylinder shell by experimental study," *Eng. Struct.*, vol. 245, p. 112862, Oct. 2021, doi: 10.1016/j.engstruct.2021.112862.
[5] J. W. Dai, Z. Qu, G. B. Nie, and C. X. Zhang, "DAMAGES OF STEEL SPACE GYMNASIUM STRUCTURES IN THE 2013 CHINA LUSHAN MS7.0 EARTHQUAKE".
[6] F. Fan, S. Z. Shen, and G. A. R. Parke, "Study of the Dynamic Strength of Reticulated Domes under Severe Earthquake Loading," *Int. J. Space Struct.*, vol. 20, no. 4, pp. 235–244, Dec. 2005, doi: 10.1260/026635105775870251.
[7] G. Nie, X. Zhu, X. Zhi, F. Wang, and J. Dai, "Study on Dynamic Behavior of Single-Layer Reticulated Dome by Shaking Table Test," *Int. J. Steel Struct.*, vol. 18, no. 2, pp. 635–649, Jun. 2018, doi: 10.1007/s13296-018-0021-2.
[8] X. Zhi, F. Fan, and S. Shen, "Elasto-plastic instability of single-layer reticulated shells under dynamic actions," *Thin-Walled Struct.*, vol. 48, no. 10–11, pp. 837–845, Oct. 2010, doi: 10.1016/j.tws.2010.04.005.
[9] F. Fan, S. Z. Shen, and G. A. R. Parke, "Theoretical and Experimental Study of Vibration Reduction in Braced Domes Using a Viscous Damper System," *Int. J. Space Struct.*, vol. 19, no. 4, pp. 195–202, Dec. 2004, doi: 10.1260/0266351043492672.
[10] G. Nie and K. Liu, "Experimental Studies of Single-Layer Reticulated Domes with Isolated Supports," *Shock Vib.*, vol. 2018, no. 1, p. 6041878, Jan. 2018, doi: 10.1155/2018/6041878.
[11] X. Zhi, F. Fan, F. Shi, and Z. Yu, "Effect of BRBs on the seismic resistance of single-layer reticulated domes," *Int. J. Steel Struct.*, vol. 13, no. 1, pp. 199–208, Mar. 2013, doi: 10.1007/s13296-013-1019-4.
[12] J. Dai, Z. Qu, C. Zhang, and X. Weng, "Preliminary investigation of seismic damage to two steel space structures during the 2013 Lushan earthquake," *Earthq. Eng. Eng. Vib.*, vol. 12, no. 3, pp. 497–500, Sep. 2013, doi: 10.1007/s11803-013-0189-6.
[13] F. Fan, J. Yan, and Z. Cao, "Stability of reticulated shells considering member buckling," *J. Constr. Steel Res.*, vol. 77, pp. 32–42, Oct. 2012, doi: 10.1016/j.jcsr.2012.04.011.
[14] S. Kato, J.-M. Kim, and M.-C. Cheong, "A new proportioning method for member sections of single layer reticulated domes subjected to uniform and non-uniform loads," *Eng. Struct.*, vol. 25, no. 10, pp. 1265–1278, Aug. 2003, doi: 10.1016/S0141-0296(03)00077-4.
[15] G. Nie, X. Zhi, F. Fan, and J. Dai, "Seismic performance evaluation of single-layer reticulated dome and its fragility analysis," *J. Constr. Steel Res.*, vol. 100, pp. 176–182, Sep. 2014, doi: 10.1016/j.jcsr.2014.04.031.
[16] T. Suzuki, T. Ogawa, and K. Ikarashi, "Elasto-Plastic Buckling Analysis of Rigidly Jointed Single Layer Reticulated Domes," *Int. J. Space Struct.*, vol. 7, no. 4, pp. 363–368, Dec. 1992, doi: 10.1177/026635119200700412.
[17] American Society of Civil Engineers, *Minimum Design Loads and Associated Criteria for Buildings and Other Structures*, 7th–16th ed. Reston, VA: ASCE, 2017.
[18] A. Whittaker, "Selecting and Scaling Earthquake Ground Motions for Performing Response-History Analyses," National Institute of Standards and Technology, GCR 11-917-15, 2011.
[19] K. Shahzada, "Seismic Risk Assessment of Buildings in Pakistan (Case Study Abbottabad City)," PhD Dissertation, University of engineering and technology, Peshawar, 2011.
[20] U. Oğuz, "Comparison of Ground Motion Scaling Methods by Considering Vertical Ground Motions," Master's thesis, Middle East Technical University, Ankara, Turkey, 2022.
[21] F. Fan, D. Wang, X. Zhi, and S. Shen, "Failure modes for single-layer reticulated domes under impact loads," *Trans. Tianjin Univ.*, vol. 14, no. S1, pp. 545–550, Oct. 2008, doi: 10.1007/s12209-008-0094-7.
[22] X.-M. Jiang, H. Chen, and J. Y. R. Liew, "Spread-of-plasticity analysis of three-dimensional steel frames," *J. Constr. Steel Res.*, vol. 58, no. 2, pp. 193–212, Feb. 2002, doi: 10.1016/S0143-974X(01)00041-4.